Sakarya University Journal of Science

ISSN : 2147-835X
Publisher : Sakarya University

Vol. 28, No. 2, 344-352, 2024
DOI: https://doi.org/10.16984/saufenbilder.1350708

Research Article

Optical Signal Investigation of Monolayer MoS_2 Grown Via Glass-Assisted CVD On Patterned Surfaces

Aydan Yeltik

TOBB University of Economics and Technology, Faculty of Engineering, Department of Material Science and Nanotechnology Engineering, Ankara, Türkiye, ayeltik@etu.edu.tr

ARTICLE INFO

Keywords:
2D Material
Transition Metal
Dichalcogenide
Photoluminescence
Chemical Vapor Deposition
Patterned Surface

Article History:
Received: 27.08.2023
Accepted: 05.01.2024
Online Available: 24.04.2024

ABSTRACT

Enhancing photoluminescence (PL) in single-layer transition metal dichalcogenides has garnered significant interest, particularly for advancing high-performance 2D electronics and optoelectronics. The combination of surface engineering and contemporary growth methods has provided a platform for investigating optical signals. In this study, we present variations in PL and Raman signals of single-layer MoS_2 flakes grown conformally using the glass-assisted CVD method on square-patterned surfaces with varying well depths. PL spectroscopy revealed a systematic and pronounced enhancement in intensities as the valley thickness decreased from 285 nm to 225 nm. Conversely, for the hill regions of the samples, the PL intensity initially increased with decreasing valley thickness and then decreased, despite the hill regions having a constant thickness of 300 nm. On the other hand, PL maps did not exhibit a systematic dependence of intensities on the hill-valley thickness distinction, contrary to expected results based on literature data for similar materials on flat surfaces. The origin of the intensity oscillations was attributed to possible mechanisms, including thickness-dependent interference and strain-related exciton funneling effects. Additionally, Raman measurements revealed irregular variations in intensity in hill regions, dependent on the thicknesses of the underlying SiO_2 layers. Furthermore, we observed that the sizes of the flakes increased as the well depths of the underlying patterned surface decreased. This phenomenon might be attributed to alterations in the carrier gas flow pattern and varying temperature gradients between the hills and valleys. These results hold substantial potential to open new avenues for the integration of 2D transition metal dichalcogenides into on-chip electronic and optoelectronic devices.

1. Introduction

Transition metal dichalcogenide (TMD) materials have attracted considerable attention due to their advantageous properties, such as a tunable direct bandgap, high carrier mobility, and stability, crucial for future electronic and optoelectronic applications [1–6].

Previous studies have demonstrated enhanced photoluminescence (PL) in suspended graphene and MoS_2, attributing it to the reduction of detrimental interactions with underlying substrates. These interactions include nonradiative recombination, charge transfer, and various excitonic transitions [7–10]. Moreover, the dielectric surroundings around 2D materials were reported to regulate the in- and out-coupling of light, resulting in significant variations in PL and Raman intensities [11–15].

Zhang et al. examined the impact of multilayer film interference on the optical signal of single-layer MoS_2 on a flat SiO_2/Si substrate, determining that the correct SiO_2 layer thickness is crucial for improving PL and Raman intensities [16]. Similarly, Lien et al. investigated thickness-dependent interference effects for

Cite as: Yeltik A. (2024). Optical Signal Investigation of Monolayer MoS2 Grown Via Glass-Assisted CVD On Patterned Surfaces, *Sakarya University Journal of Science,* 28(2), 344-352. https://doi.org/10.16984/saufenbilder.1350708

single-layer WSe_2. They observed that the outcoupling mechanism, involving numerous reflections, leads to variations in PL signal depending on the thickness of the underlying SiO_2 surface [17]. Additionally, the dependence of the Raman signal of monolayer MoS_2 and WSe_2 on the thickness of the flat SiO_2 layer was revealed in previous studies [16, 17].

However, despite being a promising candidate among 2D TMDs with optoelectronic properties surpassing graphene and other 2D materials [18], the impact of surroundings on the optical signals of monolayer MoS_2 on patterned surfaces has not been thoroughly explored. Therefore, it remains both significant and challenging to examine the optical signal of monolayer MoS_2 based on the well depths of patterned surfaces in order to uncover the underlying mechanisms.

In this study, the impact of surface patterning on the PL and Raman signals of monolayer MoS_2 was investigated, correlating these effects with the depth of patterned wells. This variation in well depth induces changes in the surrounding dielectric environment and potentially other parameters. Patterned surfaces, featuring square arrays with varying well depths, were employed to elucidate the optical characteristics of monolayer crystals grown conformally on hill and valley regions. The properties of these flakes were predominantly investigated through atomic force microscopy (AFM), μ-PL spectroscopy, and μ-Raman spectroscopy.

By adjusting well depths, we achieved tunable and distinctive PL intensities specific to the thickness of the underlying substrate. Raman signals were also scrutinized, revealing negligible oscillatory behaviors. Furthermore, the lateral sizes of monolayer MoS_2 exhibited changes corresponding to the well depth of the patterned surfaces. The findings presented in this study demonstrate the substantial effects of patterned substrate features on the optical emission outcoupling of conformally grown monolayer MoS_2.

2. Experımental Section

2.1.Surface patterning

SiO_2 surfaces on p-type Si substrates were patterned through a photolithography process followed by plasma etching. The Karl Suss MJB4 mask aligner facilitated the photolithography, while an inductively coupled plasma (Advanced Vacuum ICP) system was utilized for SiO_2 surface patterning. Initially, after substrate cleaning, samples were spin-coated with positive photoresist AZ5214E at 4000 rpm for 40 s and subsequently annealed at 110 ^oC for 50 s. Following alignment with the mask, the samples were exposed to UV for 50 s. UV-exposed areas were then developed using AZ 351B developer, and residual components were removed by washing with DI water. A protective layer was formed by waiting for 10 min at 110 ^oC. Patterning was achieved through an ICP etching process under the conditions of 40 sccm CF_4 gas flow, 700 mW power, and 100 mTorr pressure. Etching times were set at 5 s, 10 s, and 20 s to achieve SiO_2 layer thicknesses of 285 nm (15 nm depth), 270 nm (30 nm depth), and 225 nm (75 nm depth), respectively, at the valleys.

2.2.Growth precursors and wafers

Sulphur (S) (Sigma-Aldrich 99.98%) and molybdenum (MoO_3) (SigmaAldrich 99.995%) precursors, both in powder form, were employed in amounts of 300 mg and 0.5 mg, respectively. Commercially obtained SiO_2/Si substrates with lateral dimensions of 2 cm x 2 cm and lamellas measuring 2 cm x 2 cm x 0.15 mm were used. Energy dispersive X-ray (EDX) spectroscopy analysis revealed glass atomic concentrations of 9.42% sodium, 2.45% magnesium, and 2.28% calcium.

2.3.Crystal growth

A horizontal CVD system, featuring a quartz tube with a 7 cm diameter, was utilized for the growth of monolayer MoS_2 crystals (Figure 1). The system underwent pre-cleaning by raising the temperature to 1100 °C (with a rate of increase of 12 °C/min) under a 500 sccm N_2 gas

flow at atmospheric pressure, followed by a 20-minute waiting period. Soda-lime glass lamellas were positioned on the plate inside the system, with a graphite foil placed between them to prevent cracking. The SiO_2/Si substrates were located near the lamellas, as depicted in the figure. Sulphur was placed in a quartz container, and MoO_3 was positioned on a SiO_2/Si substrate. The distance between MoO_3-S and MoO_3-the beginning point of SiO_2/Si substrates were determined as 4x and x, respectively, where x equals 4 cm. The growth conditions were maintained at 750 °C (with a rate of increase of 12 °C/min), 5 min duration, 150 sccm carrier gas flow rate, and 760 Torr pressure.

2.4.Material characterization

The Witec Alpha 300R μ-Raman and μ-PL spectroscopy system, equipped with a Zeiss objective, was employed for structural and optical analyses at room temperature. A continuous-wave laser with a 532 nm wavelength, 0.5 mW power, 1 s integration time, and a 300 nm spot size was used. Nanomagnetic Instruments AFM (tapping mode) was utilized for examining flake thickness, and 2D material morphologies were observed using the Nikon Eclipse LV100NDA microscopy system.

3. Results and Discussions

Figure 1 illustrates a schematic representation of the glass-assisted CVD MoS_2 configuration.

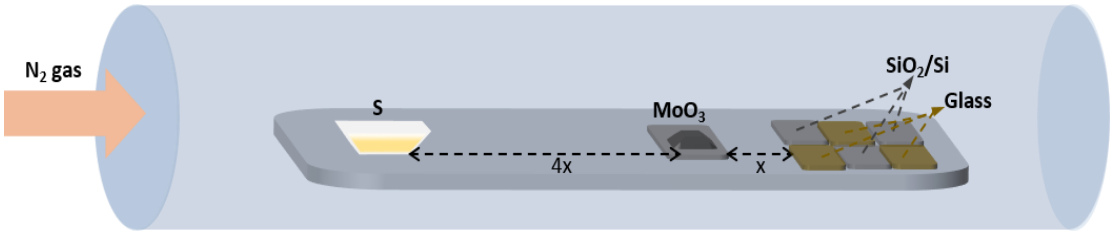

Figure 1. Schematic representation of the glass-assisted CVD configuration

The growth process was optimized for a three of which are SiO_2/Si (with one patterned surface and two flat surfaces) and the remaining three are soda-lime glasses. Monolayer MoS_2 structures were grown on square-patterned silica surfaces with varying valley thicknesses, as depicted in Figure 2(a-c). The surfaces featured square patterns spaced approximately 20 μm apart, with varying valley SiO_2 thicknesses (i.e., 285 nm, 270 nm, and 225 nm) serving as the growth substrates. To enhance the crystal growth rate, soda-lime glasses with a high sodium concentration were employed as growth promoters, aligning with findings from previous studies [19, 20]. The presence of sodium ions in the lamellas produces an intermediate product that is highly volatile compared to the melting point of MoO_3. This, in turn, lowers the growth temperature, accelerating the MoS_2 growth process [18].

The size of the triangular-shaped MoS_2 flakes increased proportionally with the rise in valley thickness, as illustrated from (c) to (a) in Figure 2. While the primary cause for this difference may be attributed to alterations in the carrier gas flow pattern, sophisticated simulations are required to validate this argument. Additionally, the formation of larger flakes could be traced back to an elevated growth rate, potentially influenced by the varying temperature gradients between the hills and valleys [21].

In Figure 3(a-c), AFM images and corresponding thickness profiles of the flakes grown on the surfaces with three distinct valley thicknesses are presented. These profiles reveal that the thickness of the flakes is ~0.7 nm, a value consistent with literature results for monolayer MoS_2 [22]. Moreover, measurements on the valley pattern regions indicated similar thicknesses of around 0.7 nm, pointing towards conformal growth on the studied surfaces. The heightened surface wettability resulting from sodium content in the growth process aligns with the anticipated outcome of conformal growth in these samples [23]. Particles located at the edge of the crystal are often responsible for a sharp peak in the AFM line profiles, which is a

common phenomenon for CVD-grown MoS_2 without H_2 gas [24, 25]. At the edges of a MoS_2 flake, atoms experience a different environment compared to the interior of the crystal. The coordination and bonding of atoms at the edge are altered, resulting in a modified electronic structure and, consequently, an increase in thickness at the edge.

Figure 2. Monolayer MoS_2 flakes on patterned surfaces with valley thicknesses of (a) 285 nm (15 nm depth), (b) 270 nm (30 nm depth), and (c) 225 nm (75 nm depth)

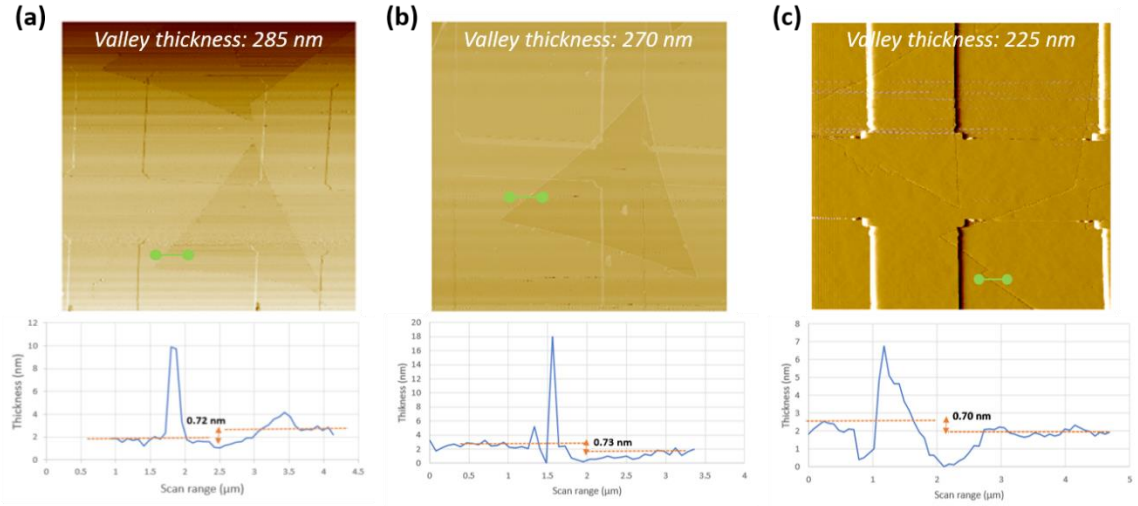

Figure 3. AFM images of MoS_2 materials on patterned surfaces with valley thicknesses of (a) 285 nm, (b) 270 nm, and (c) 225 nm, accompanied by the corresponding thickness profiles

Monolayer MoS_2 materials were further examined through µ-PL and µ-Raman spectroscopy. Figure 4(a-c) present PL intensity maps obtained with a 532-nm excitation wavelength from the flakes grown on the patterns with decreasing valley thicknesses (increasing well depths). The corresponding optical microscopy (OM) images of the flakes are inset in the figures. The PL intensities did not exhibit a systematic dependence on the hill-valley thickness distinction, which is not an expected result considering literature data for similar materials on flat surfaces [16, 17].

Zhang et al. previously explored the influence of multilayer film interference on the optical signal of monolayer MoS_2 on SiO_2/Si substrate and revealed that the proper SiO_2 layer thickness is important to enhance the PL and Raman intensities [16]. However, contrary to the presented results here at the 532-nm excitation wavelength, they observed PL enhancement with increasing thickness of flat SiO_2 in the spectral region we focused on (225 to 285 nm).

Similarly, Lien et al. investigated thickness-dependent interference effects for single-layer WSe_2, revealing that the PL signal exhibited almost unvarying behavior between 225 and 285 nm thickness of the underlying SiO_2 layer. This behaviour was attributed to the outcoupling mechanism with multiple reflections [17].

Figure 5 presents separate PL intensity curves from the valley and hill regions. A systematic and pronounced enhancement in PL intensities was observed with decreasing valley thickness. Conversely, for the hill regions of the samples, the PL intensity initially increased with decreasing valley thickness and then decreased, despite the hill regions having the same thicknesses in these samples. The PL peak positions were determined to be 1.793, 1.818, and 1.815 eV for SiO_2 valley thicknesses of 285 nm, 270 nm, and 225 nm, respectively (Figure 5(a)). Similarly, in the same order, the PL peak positions were found to be 1.794, 1.819, and 1.817 eV (Figure 5(b)) for SiO_2 hill regions with a constant thickness of 300 nm. The deconvoluted data and peak positions for each PL curve in Figure 5 are also presented in the supplementary file (Figure S1).

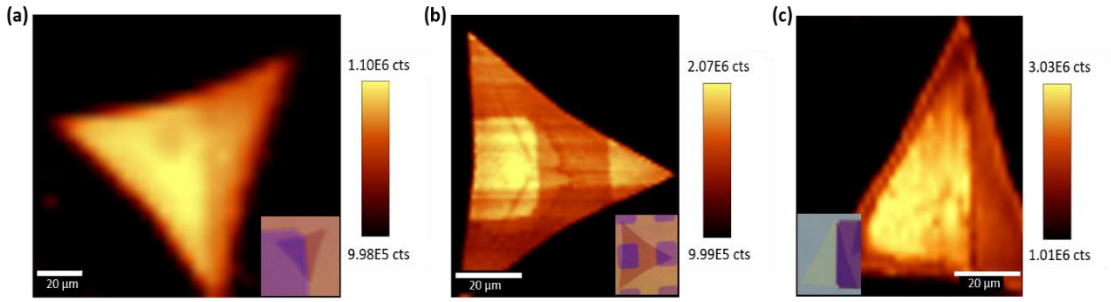

Figure 4. PL intensity maps of single-layer flakes on patterned surfaces with valley thicknesses of (a) 285 nm, (b) 270 nm, and (c) 225 nm. The insets show OM images of the flakes

In related literature, Wang et al. explored 2D materials on zero and non-zero Gaussian structures, such as trench and donut-like geometries [26]. They noted significant PL peak intensity changes between the valley and hill areas on both zero and non-zero Gaussian structures, attributing these variations to thickness-dependent interference. While over non-zero Gaussian regions, 2D materials grew under strain, resulting in a significant redshift at the PL peak wavelength, only minor meV shifts were observed in the PLs of our study obtained from the valley-hill regions of each sample.

Though exciton funneling effects were not expected to be evident in this study, strain-induced exciton funneling still might be the underlying mechanism for these nonuniform PL variations, yet there need to be more investigation including high resolution data on these findings especially from the vicinity of the pattern edges. Additionally, the location of the flakes on the patterns and the carrier gas flow pattern, as noted earlier for size distribution variations, should be subjects of continued investigation for a more comprehensive understanding of these interesting optical results.

Raman spectral peaks corresponding to the E^1_{2g} in-plane and A^1_g out-of-plane modes at valley points were observed at around 384 and 404 cm^{-1}, 381 and 400 cm^{-1}, 383 and 402 cm^{-1} for SiO_2 valley thicknesses of 285 nm, 270 nm, and 225 nm, respectively (Figure 6(a)). The change in the Raman modes, measured as $\triangle$=19-20 cm^{-1}, indicated the growth of monolayer MoS_2 on the studied patterned surfaces [27]. Similarly, Raman peaks at hill points were obtained at around 383 and 402 cm^{-1}, 382 and 402 cm^{-1}, 383 and 402 cm^{-1} for SiO_2 valley thicknesses of 285 nm, 270 nm, and 225 nm, respectively (Figure 6(b)). The mode difference was measured as $\triangle$=19-20 cm^{-1}, indicating monolayer growth of MoS_2. The Raman peak intensities remained approximately constant without a systematic variation particularly at the hill points.

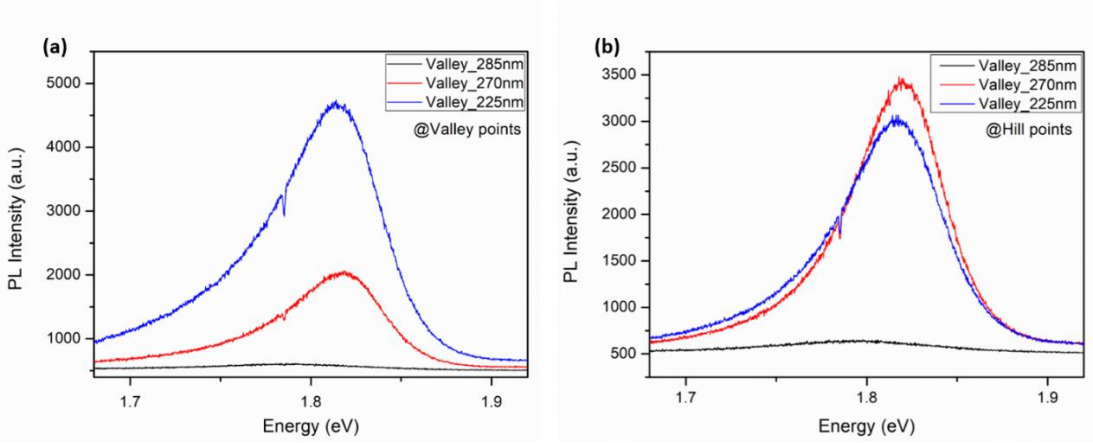

Figure 5. PL spectra from both the (a) valley and (b) hill regions of the samples with varying SiO_2 layer thicknesses at valleys. The hills correspond to 300 nm thick SiO2 layer on Si for all the samples

Notably, there was no considerable spectral difference observed between the valley and hill regions with changes in underlying SiO_2 thickness. The 2LA mode observed at around 450 cm^{-1} in the second-order Raman resonance, which involves longitudinal acoustic phonons, is attributed to the in-plane collective motions of atoms within the MoS_2 lattice [28]. The absence of additional Raman peaks suggests that glass components are not responsible for the varying intensity of PLs. As the study's parameters were consistently maintained, any potential doping effect is anticipated to be uniform across both hills and valleys. On the other hand, Zhang et al. reported enhanced modes of monolayer MoS_2 Raman signal from 225 nm to both 270 nm and 285 nm thicknesses of flat SiO_2 capping layers [16]. In addition, Lien et al. observed oscillatory behaviour in the Raman signal of single-layer WSe_2 between 225 and 285 nm thicknesses of underlying SiO_2, attributed to multiple-reflection light outcoupling [17]. The optical signals of monolayer MoS_2 on the patterned surfaces in this study displayed distinct variation profiles with underlying SiO_2 thickness, contrary to literature values that typically use flat surfaces. These results suggest characteristic features specific to the studied patterned platform for monolayer MoS_2.

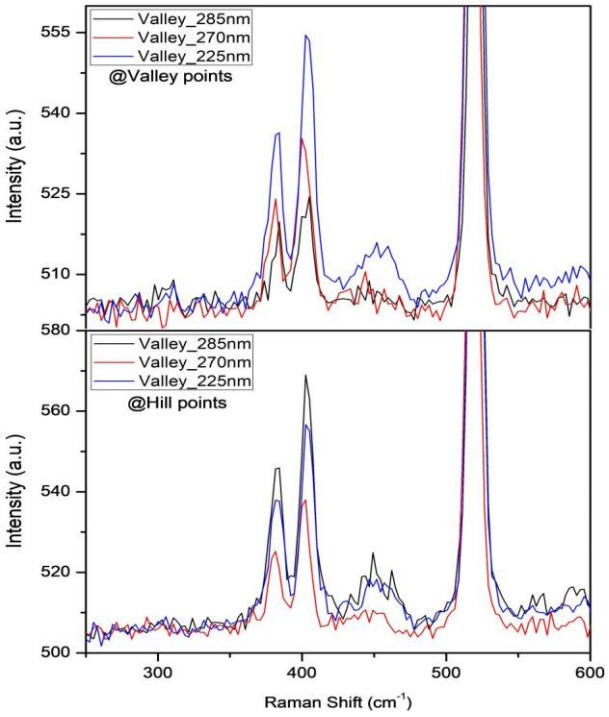

Figure 6. Raman spectra from both the (a) valley and (b) hill regions of the samples with varying SiO_2 layer thicknesses at valley

4. Conclusions and Discussion

In conclusion, this study demonstrates that the optical signals of single-layer MoS_2, grown conformally on square-patterned surfaces via glass-assisted CVD, exhibit distinct characteristics compared to those on flat platforms. Specifically, in samples with valley thicknesses of 285 nm and 270 nm, the PL intensity in square hills appeared higher than in valleys, whereas the opposite result was obtained in structures with a valley thickness of 225 nm.

Furthermore, the PL from the valley points enhanced as the valley thickness decreased from 285 nm to 225 nm, while the PL intensity initially increased for the hill regions with decreasing valley thickness and then diminished, despite the hill regions having a constant thickness of 300 nm. The oscillations in PL might be attributed to potential mechanisms, including thickness-dependent interference and strain-related exciton funneling effects.

Notably, the Raman signals of the samples did not exhibit a systematic behaviour at the hill points. Additionally, the lateral dimensions of the monolayer MoS_2 flakes showed varying behavior on the patterned surfaces with changes in well depth. This variability is likely a result of alterations in the carrier gas flow pattern and varying temperature gradients between the hills and valleys. These findings may pave the way for novel strategies in the effective integration of 2D TMDs into nanoelectronic and optoelectronic devices. Consequently, follow-up studies are of high significance to reveal the underlying mechanisms of the results presented in this study.

Article Information Form

Acknowledgments
The author would like to thank Prof. Nihan Kosku Perkgoz and Prof. Feridun Ay for their valuable support.

Funding
The study was supported by The Scientific and Technological Research Council of Turkey Project Number: 121M601.

Authors' Contribution
Conceptualization, A.Y.; methodology, A.Y.; data curation, A.Y.; writing—original draft preparation, A.Y.; writing—review and editing, A.Y. All authors have read and agreed to the published version of the manuscript.

The Declaration of Conflict of Interest/ Common Interest
No conflict of interest or common interest has been declared by the author.

The Declaration of Ethics Committee Approval
This study does not require ethics committee permission or any special permission.

The Declaration of Research and Publication Ethics
The authors of the paper declare that they comply with the scientific, ethical and quotation rules of SAUJS in all processes of the paper and that they do not make any falsification on the data collected. In addition, they declare that Sakarya University Journal of Science and its editorial board have no responsibility for any ethical violations that may be encountered, and that this study has not been evaluated in any academic publication environment other than Sakarya University Journal of Science.

References

[1] W. Zhu, T. Low, H. Wang, P. Ye, X. Duan, “Nanoscale electronic devices based on transition metal dichalcogenides”, 2D Materials, vol. 6, no. 3, pp. 1–18, 2019.

[2] T. J. Ko, M. Wang, C. Yoo, E. Okogbue, M. A. Islam, H. Li, M. S. Shawkat, S. S. Han, K. H. Oh, Y. Jung, “Large-area 2D TMD layers for mechanically reconfigurable electronic devices”, Journal of Physics D: Applied Physics, vol. 53, no. 31, pp. 1–27, 2020.

[3] E. Singh, P. Singh, K. S. Kim, G. Y. Yeom, H. S. Nalwa, “Flexible molybdenum disulfide (MoS2) atomic layers for wearable electronics and optoelectronics”, ACS Applied Materials & Interfaces, vol. 11, no. 12, pp. 11061–11105, 2019.

[4] J. Cheng, C. Wang, X. Zou, L. Liao, “Recent advances in optoelectronic devices based on 2D materials and their heterostructures”, Advanced Optical Materials, vol. 7, no. 1, pp. 1–15, 2019.

[5] S. Aftab, M. Z. Iqbal, S. Hussain, H. H. Hegazy, M. A. Saeed, “Transition metal dichalcogenides solar cells and integration with perovskites: A review”, Nano Energy, vol. 108, no. 108249, pp. 1–17, 2023.

[6] R. Sharma, R. Laishram, B. K. Gupta, “A Review on MX2 (M = Mo, W and X = S, Se) layered material for opto-electronic devices”, Advances in Natural Sciences: Nanoscience and Nanotechnology, vol. 13, no. 023001, pp. 1–18, 2022.

[7] S. Berciaud, S. Ryu, L. E. Brus, T. F. Heinz, “Probing the lntrinsic properties of exfoliated graphene: Raman spectroscopy of free-standing monolayers”, Nano Letters, vol. 9, no. 1, pp. 346–352, 2009.

[8] D. Sercombe, S. Schwarz, O. Del Pozo-Zamudio, F. Liu, B. J. Robinson, E. A. Chekhovich, I. I. Tartakovskii, O. Kolosov, A. I. Tartakovskii, “Optical investigation of the natural electron doping in thin MoS 2 films deposited on dielectric substrates”, Scientific Reports, vol. 3, no. 3489, pp. 1–6, 2013.

[9] K. F. Mak, C. Lee, J. Hone, J. Shan, T. F. Heinz, “Atomically thin MoS2: A new direct-gap semiconductor”, Physical Review Letters, vol. 105, no. 13, p. 136805, Sep. 2010.

[10] N. Scheuschner, O. Ochedowski, A. M. Kaulitz, R. Gillen, M. Schleberger, J. Maultzsch, “Photoluminescence of freestanding single- and few-layer MoS 2”, Physical Review B - Condensed Matter and Materials Physics, vol. 89, no. 12, pp. 2–7, 2014.

[11] H. Fang, H. A. Bechtel, E. Plis, M. C. Martin, S. Krishna, E. Yablonovitch, A. Javey, “Quantum of optical absorption in two-dimensional semiconductors”, Proceedings of the National Academy of Sciences of the United States of America, vol. 110, no. 29, pp. 11688–11691, 2013.

[12] S. L. Li, H. Miyazaki, H. Song, H. Kuramochi, S. Nakaharai, K. Tsukagoshi, “Quantitative raman spectrum and reliable thickness identification for atomic layers on insulating substrates”, ACS Nano, vol. 6, no. 8, pp. 7381–7388, 2012.

[13] D. Yoon, H. Moon, Y. W. Son, J. S. Choi, B. H. Park, Y. H. Cha, Y. D. Kim, H. Cheong, “Interference effect on Raman spectrum of graphene on SiO2 /Si”, Physical Review B - Condensed Matter and Materials Physics, vol. 80, no. 12, pp. 1–6, 2009.

[14] F. G. Aras, J. Avad, A. Yeltik, “Glass-assisted chemical vapor deposition-grown monolayer MoS2: Effective control of size distribution via surface patterning”, Physica Status Solidi, vol. 219, no. 24, pp. 1–8, 2022.

[15] F. G. Aras, A. Yeltik, “Role of gas flow direction on monolayer MoS2 growth on patterned surfaces via CVD”, Semiconductor Science and Technology, vol. 38, no. 015013, pp. 1–8, 2023.

[16] H. Zhang, Y. Wan, Y. Ma, W. Wang, Y. Wang, L. Dai, “Interference effect on optical signals of monolayer MoS2”, Applied Physics Letters, vol. 107, no. 10, pp. 1–5, 2015.

[17] D.-H. Lien, J. S. Kang, M. Amani, K. Chen, M. Tosun, H. -P. Wang, T. Roy, M. S. Eggleston, M. C. Wu, M. Dubey, S. -C. Lee, J. -H. He, A. Javey, “Engineering light outcoupling in 2D materials”, Nano Letters, vol. 15, no. 2, pp. 1356–1361, 2015.

[18] F. G. Aras, A. Yilmaz, H. G. Tasdelen, A. Ozden, F. Ay, N. K. Perkgoz, A. Yeltik, “A review on recent advances of chemical vapor deposition technique for monolayer transition metal dichalcogenides (MX2: Mo, W; S, Se, Te)”, Materials Science in Semiconductor Processing, vol. 148, no. 106829, pp. 1–22, 2022.

[19] G. U. Özküçük, C. Odacı, E. Şahin, F. Ay, N. K. Perkgöz, "Glass-assisted CVD growth of large-area MoS2, WS2 and MoSe2 monolayers on Si/SiO2 substrate", Materials Science in Semiconductor Processing, vol. 105, no. 104679, pp. 1–7, 2020.

[20] I. W. Lisheshar, "Hybrid supercapacitors based on two dimensional materials: MXenes, Graphene and TMDCs", Eskisehir Technical University, 2019.

[21] Z. Cheng, M. Xia, S. Liu, R. Hu, G. Liang, S. Zhang, "Role of rough substrate on the growth of large single-crystal MoS2 by chemical vapor deposition", Applied Surface Science, vol. 476, pp. 1008–1015, May 2019.

[22] H. Kim, W. Kim, M. O. Brien, N. Mcevoy, "Optimized single-layer MoS2 field-effect transistors by non-covalent functionalisation", Nanoscale, vol. 10, no. 37, pp. 17557–17566, 2018.

[23] S. Li, "Salt-assisted chemical vapor deposition of two-dimensional transition metal dichalcogenides", iScience, vol. 24, no. 11, p. 103229, 2021.

[24] Y. Yoo, Z. P. Degregorio, J. E. Johns, "Seed crystal homogeneity controls lateral and vertical heteroepitaxy of monolayer MoS2 and WS2", Journal of The American Chemical Society, vol. 137, no. 45, pp. 14281–14287, 2015.

[25] H. Liu, Y. Zhu, Q. Meng, X. Lu, S. Kong, Z. Huang, P. Jiang, X. Bao, "Role of the carrier gas flow rate in monolayer MoS2 growth by modified chemical vapor deposition", Nano Research, vol. 10, no. 2, pp. 643–651, 2017.

[26] K. Wang, A. A. Puretzky, Z. Hu, B. R. Srijanto, X. Li, N. Gupta, H. Yu, M. Tian, M. Mahjouri-Samani, X. Gao, A. Oyedele, C. M. Rouleau, G. Eres, B. I. Yakobson, M. Yoon, K. Xiao, D. B. Geohegan, "Strain tolerance of two-dimensional crystal growth on curved surfaces", Science Advances, vol. 5, no. 5, pp. 1–11, 2019.

[27] T. Yang, X. Huang, H. Zhou, G. Wu, T. Lai, "Excitation mechanism of A1g mode and origin of nonlinear temperature dependence of Raman shift of CVD-grown mono- and few-layer MoS2 films", Optics Express, vol. 24, no. 11, p. 12281, 2016.

[28] H. Guo, Y. Sun, P. Zhai, J. Zeng, S. Zhang, P. Hu, H. Yao, J. Duan, M. Hou, J. Liu, "Resonant Raman spectroscopy study of swift heavy ion irradiated MoS2", Nuclear Instruments and Methods in Physics Research B, vol. 381, pp. 1–5, 2016.